The enhancement of Raman scattering, resonance Raman scattering, and fluorescence from molecules adsorbed on a rough silver surface

D. A. Weitz and S. Garoff

Exxon Research and Engineering Company, Linden, New Jersey 07036

J. I. Gersten

Department of Physics, City College of the City University of New York, New York, New York 10031

A. Nitzan

Department of Chemistry, Tel Aviv University, Tel Aviv, Israel
(Received 16 August 1982; accepted 18 January 1983)

The enhancements of normal Raman scattering, resonance Raman scattering, and fluorescence from molecules adsorbed on identical, well-characterized, silver-island films are reported. The enhancement arises from the electromagnetic interaction between the molecules and the electronic plasma resonance of the silver islands. A hierarchy of enhancement ratios is found, with typical values of 10^5 for RS, 10^3 for RRS and 10^{-1} to 10 for fluorescence, depending on the quantum yield of the molecular fluorescence. A model, developed on heuristic grounds and substantiated using the density matrix formalism, describes the light scattering processes and the effects of the plasma resonance. This model presents a unified picture of the surface-induced enhancement effects and is consistent with the experimental values. The comparison of all the forms of optical scattering leads to a complete determination of the role of the plasma resonances in the various portions of the scattering process. The excitation of the electronic plasma resonance results in an increased local field at the molecules leading to an increased excitation or absorption rate. Similarly, the excitation of the plasma resonance by the molecular emission dipole results in an increase in the radiative decay rate. However, the electromagnetic coupling of the molecule to the plasma resonance also adds an additional damping channel which can result in a reduction of the absorption or excitation rate as well as the emission yield. The resultant balance of these processes leads to the hierarchy in the measured enhancements. The hierarchy of enhancements is also shown to have important spectroscopic consequences.

I. INTRODUCTION

The optical properties of molecules can be dramatically altered when they are adsorbed on or near some rough metal surfaces. While considerable attention has been focused on the enormous increase in the Raman scattering (RS) from adsorbates on such surfaces, there still remains some controversy as to the origin of surface-enhanced Raman scattering (SERS).[1] One effect that makes a substantial contribution to the enhancement, in most instances, is the electromagnetic interaction among the optical fields, the adsorbed molecules, and the electronic plasma resonances localized on the roughness features of the metal surface.[2] The role of these electromagnetic interactions on the enhancement of the RS from adsorbed molecules has been widely studied,[2-8] but much less studied are their substantial effects on other linear optical scattering processes, including fluorescence and resonance Raman scattering (RRS). However, a detailed understanding of these effects is also crucial, both to exploit the surface enhancement for spectroscopic purposes, and to fully understand the role played by the electromagnetic interactions on the enhancement of optical scattering phenomena.

In this paper, we examine the relative surface enhancements for normal and resonance Raman scattering as well as fluorescence, and present a unified picture of the effects of the electromagnetic interactions on all of these inelastic scattering processes. In each case, we make a quantitative comparison of the signal from the adsorbates in an electromagnetically inert environment to that from an equivalent coverage on a silver-island film. Island films make excellent substrates for this study, as they can be simply and reproducibly fabricated, and their intrinsic optical properties are easy to measure and well studied.[9] Electromagnetic interactions appear to dominate their optical properties allowing a straightforward characterization of their behavior in terms of their absorption.[10,11] We find that there is a hierarchy of enhancements, with normal RS enhanced by $\sim 10^5$ while RRS is enhanced by $\sim 10^3$. The enhancement of fluorescence depends sensitively on the quantum efficiency (QE) for fluorescence of the molecule in the electromagnetically inert environment. If this is low (<0.01), the fluorescent emission is enhanced by ~ 10; however, if it is high (~ 1), the fluorescent emission is actually diminished on the silver-island film.

We present a simple model which treats all the inelastic scattering processes in a unified fashion, and successfully accounts for our observations. The model is based upon the theory of the electromagnetic interactions with an isolated spheroid that has been used to treat SERS,[2-5] fluorescence,[12,13] and photochemical reactions[14] near rough metal surfaces. This theory has been successfully used to guide the interpretation of a

 0021-9606/83/095324-15$2.10

variety of experimental observations including the SERS excitation profile on island films[10] and microlithographically prepared surfaces,[6] as well as measurements of fluorescence[15–17] and fluorescence lifetime.[18] In this paper, we generalize the theory to explicitly include the optical scattering processes that occur when the adsorbate is excited into a molecular resonance. In this case, the silver island supplies an additional decay mechanism, which arises from the possibility of very rapid transfer of the excitation from the molecule to the island via the excitation of a localized plasma resonance. The decay of this excitation can be either nonradiative, which results in absorption in the silver island, or radiative, which results in emission of a photon. The importance of this increased decay rate has been measured explicitly for fluorescence emission from molecules on silver-island films, where the fluorescent lifetime was found to be decreased by up to three orders of magnitude.[18] When the role of this additional decay channel is properly included for all scattering processes that involve a resonance excitation of the molecule, the theory can be successfully applied to account for the observed behavior of the island films.

The fundamental goal of this paper is to provide a *unified* picture of all the linear optical scattering processes from molecules adsorbed on rough metal surfaces. The enhancement of normal RS has been studied extensively to date, while the effects of the rough metal on both RRS and fluorescence have been investigated to a lesser degree. However, in this work we have studied each scattering phenomenon on identical, optically well-characterized, island-film surfaces, allowing us to make detailed comparisons between the various scattering processes. This not only provides a clear physical picture of the electromagnetic effects of the rough surface, but also affords considerable new insight into the details of the scattering processes. Similarly, the goal of the theoretical treatment presented in this paper is to provide a unified description of the effects of the electromagnetic interactions with the surface. There have been numerous treatments of SERS using the electromagnetic interactions with a dielectric spheroid,[1–5] and the spheroid calculations have also been applied theoretically to treat fluorescence of adsorbed molecules.[12,13]

In addition, a model for fluorescence from a molecule in an inert environment, which is similar in some of its fundamental aspects to portions of the model used in this paper, has been qualitatively extended to account for some observations of fluorescence on smooth and rough silver surfaces.[16] However, the experiments and theoretical discussion dealt only with the case of fluorescence from adsorbates with a low QE. In this paper, we show that the value of the QE of the adsorbate has important consequences in the enhancement of fluorescence, and can, in fact, change the observed enhancement into a decrease as the QE increases. Furthermore, in this paper, we consider the enhancement of the other optical properties, and include these scattering processes in our model, which accounts for the surface-induced properties in a more complete and detailed fashion. Therefore, the consequences of a varying QE of the free molecule are included in a consistent manner and we are able to successfully account for our important observation of a hierarchy of enhancement ratios, as well as provide a clear theoretical description of the effects of the surface on each portion of the optical scattering processes.

Besides providing a more complete picture of the electromagnetic interactions near rough metal surfaces, our results have important implications for spectroscopic applications. The observed hierarchy of enhancements, which is not unique to island films but should also apply to other rough surfaces, has obvious advantages for spectroscopy. Normal RS is an inherently weak process, and all the possible increase in signal is beneficial. In contrast, RRS is inherently more intense but is often obscured by fluorescence. Thus, the enhancement of the RRS, combined with the decrease in the fluorescence in the case of high QE, can result in a relative increase of as much as 10^4 for RRS compared to fluorescence which can be of equal importance to the enhancements themselves. Finally, the increase in the enhancement of fluorescence as the inherent molecular QE decreases is also optimal for spectroscopic applications.

The remainder of the paper is arranged as follows: The next section is a presentation of our experimental techniques and is followed by a section presenting a detailed discussion of the results for each of the forms of light scattering: Normal RS, RRS, and fluorescence; as well as a discussion of potential spectroscopic implications. Section IV contains a presentation of our theory and begins with a physical model of the light scattering processes, developed on heuristic grounds. This is then justified using a more formal density matrix treatment, and is extended to include the surface-induced effects. This theory is used as a guide in developing a model applicable to island films, which is compared to the experimental results in Sec. V. Finally, Sec. VI presents a conclusion and summary of our results.

II. EXPERIMENT

The island films are made by thermally evaporating 50 Å of silver at a rate of 1 Å/s in a cryopumped vacuum system at pressures of $\sim 10^{-6}$ Torr. When the polished silica substrates are heated to 150 °C during the evaporation, the films consist of islands, which are roughly circular in cross section, typically 200 Å in diameter, and cover 30%–40% of the surface, as shown by high resolution electron micrographs. The absorption spectrum of the films, which has a large, well defined peak at ~ 440 nm due to the excitation of the electronic plasma resonances, serves as direct measure of the strength of the electromagnetic interactions, and can be used to characterize the optical behavior of the film.[10]

All the optical measurements are made using a backscattering geometry with laser radiation from an Ar^+ or Kr^+ ion laser. The laser intensity is maintained at sufficiently low levels to insure that there is no laser-induced decay of the signal due to surface or adsorbate photodegradation. The enhancement measurements are made by comparing the signal of the light scattering from the molecules on the island film to that of the same number of

molecules in an electromagnetically inert environment.

The silver-island films are exposed to the atmosphere before the adsorbate is applied, and are most likely coated with a thin oxide layer. The adsorbates are applied by a dipping technique from a volatile solvent which produces reasonably uniform coverage controlled by the concentration of the adsorbate in the solvent.[19] For the normal RS measurements, we use *p*-nitrobenzoic acid in ethanol, which is chemisorbed as *p*-nitrobenzoate as determined by the RS spectrum.[20] For the RRS and the fluorescence measurements the dye molecules rhodamine 6G (R6G) and basic fuchsin (BF) are both used as adsorbates. In both cases, the molecules are probably physisorbed, as both their Raman and fluorescent spectra are similar on the island films and on bare silica substrates.

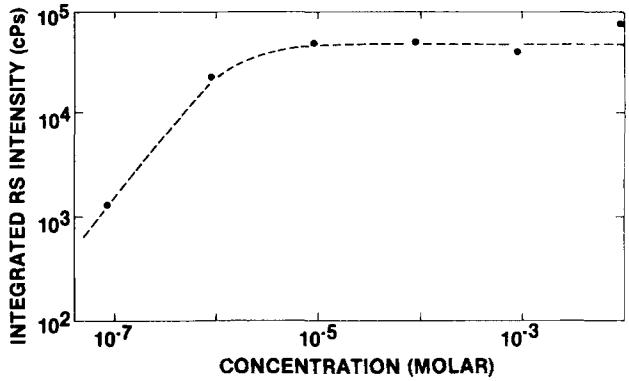

FIG. 2. SERS intensity of the 1596 cm^{-1} band of *p*-nitrobenzoate on an island film as a function of the concentration of *p*-nitrobenzoic acid in the ethanolic dipping solution.

III. RESULTS

A. Normal Raman scattering

Excellent SERS spectra of *p*-nitrobenzoate are obtained for films dipped into 10^{-3} M solutions as shown in Fig. 1(A). Confirmation that the adsorbate is *p*-nitrobenzoate is determined by comparing the SERS spectrum with that of *p*-nitrobenzoate in an ethanol solution made basic with the addition of NaOH. This spectrum is also shown for comparison in Fig. 1(B), where we have numerically subtracted the contribution of the solvent bands. All the enhancement measurements for RS are made on the sharp ring mode at 1596 cm^{-1}.

A measure of the surface coverage of *p*-nitrobenzoate on the island film is obtained by analogy with the techniques used for inelastic electron tunneling spectroscopy (IETS).[21] The SERS intensity is measured as the concentration of *p*-nitrobenzoic acid in ethanol used for the dipping is changed over six decades. As shown in Fig. 2, at low concentrations, the SERS signal increases monotonically with concentration. However, at about 10^{-5} M, the signal levels off and remains essentially constant for all higher concentrations. In analogy to the IETS work, we interpret this as the formation of a monolayer coverage, beyond which further chemisorption of *p*-nitrobenzoate is not possible. The surface coverage of a monolayer of benzoate on alumina has been measured using radioactive isotope detection techniques to be $\sim 6\times10^{14}$ molecules/cm^2 (Ref. 21), and we take this value as a reasonable approximation to the saturation coverage of the silver-island films. Using the high resolution electron micrographs, we are able to obtain a reasonable estimate of the effective area of silver covered by *p*-nitrobenzoate molecules contributing to the SERS signal.

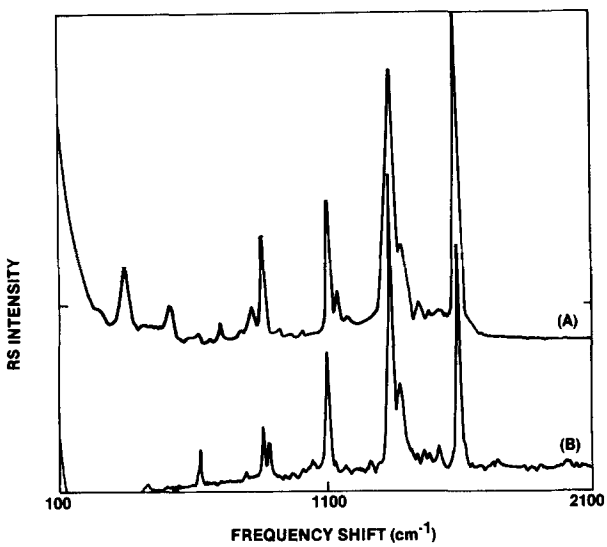

FIG. 1. RS spectra of *p*-nitrobenzoate using 515 nm excitation, (A) adsorbed on a silver-island film and (B) in a 0.25 M solution in basic ethanol, with the solvent bands numerically subtracted. Each spectrum is individually normalized.

The RS cross section without enhancement is measured using a 0.25 M solution of *p*-nitrobenzoate in a basic ethanolic solution. The identical optical scattering geometry, beam spot size, and laser power is used with the liquid contained in a 1 mm thick cuvette. The signal obtained is corrected for the decrease in collection solid angle due to the index of refraction of the bulk liquid. By comparing the signals from the island film to that of the *p*-nitrobenzoate in solution, we obtain an average enhancement per molecule of $\sim 10^5$ for normal RS on the island films. This measurement was made using 5145 Å excitation, and represents the peak enhancement for the island films used, as determined from the measured excitation spectrum.[10]

B. Resonant Raman scattering

The adsorbates used in the enhancement measurements for RRS are dye molecules which have a strong molecular absorption at roughly the same energy as the plasma resonance of the silver-island film. Application of these molecules to the island films results in dramatic changes in the absorption profile of the coated film as the coverage is increased due to the large alterations in the field configurations in and around the island.[22–24] To avoid these complications, the enhancement measurements are made using very low coverages, where the dye coating is so dilute that the dielectric function of the surface layer is essentially that of air, and the

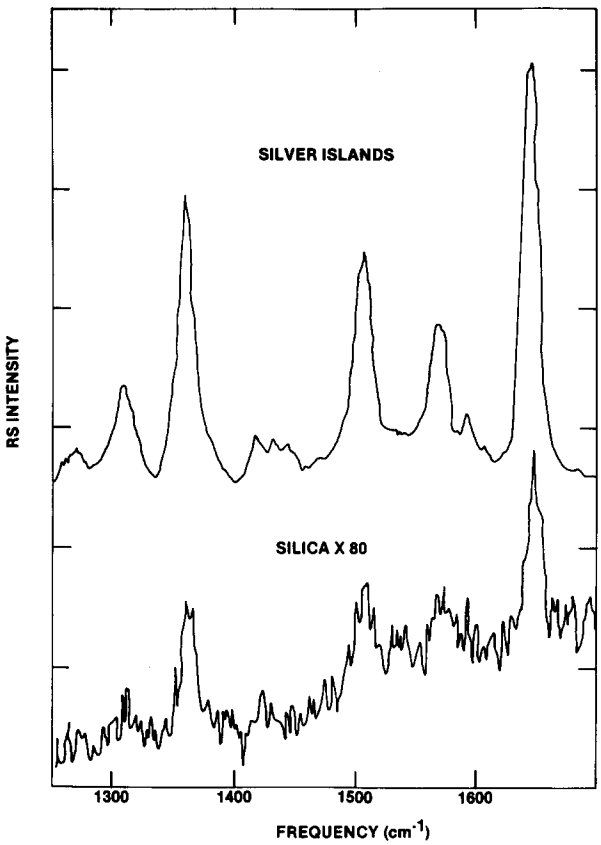

FIG. 3. Portion of the RRS spectrum of R6G adsorbed on a silver-island film and a silica substrate using 488 nm excitation.

absorption spectra of the coated films are unchanged from the spectra of either the uncoated films or those coated with a nonabsorbing molecule such as *p*-nitrobenzoate. Low coverages of R6G and BF are obtained by using a 10^{-5} M concentration dipping solution. Since the molecular resonance provides a large enough cross section to detect the RRS from submonolayer coverage on a bare silica substrate the enhancement is measured directly by comparing the signal levels from an island film and a bare silica surface which is essentially electromagnetically "inert ." Since the dye molecules are physisorbed, dipping the substrates under identical conditions produces approximately equal coverages, independent of the surface.[19] This has been verified for numerous surfaces, and is confirmed in this case by comparing the fluorescence spectra of island films and bare silica substrates coated under identical dipping conditions from a series of dye concentrations. A detailed study of the fluorescence spectra of dye molecules on silica surfaces has shown a monotonic increase in the wavelength of the peak of the fluorescence emission as the concentration of the adsorbate in the dipping solution is increased.[19] This is due to the shift in the fluorescence spectrum caused by the increasing formation of aggregates as the coverage increases. The peak of the fluorescence from a silver-island film occurs at the same wavelength as that from a silica surface when they are dipped under identical conditions, and the peaks shift the same amount as the concentration of the dipping solution is changed. This provides experimental evidence that, for dye molecules, approximately equal coverages of adsorbates can be achieved for the silver-island films and bare silica substrates.

A typical example of the RRS spectra obtained for slightly higher coverages of R6G on both an island film and a bare silica substrate is shown in Fig. 3. For the lower coverage on silica, more extensive signal averaging is required to obtain good statistics. The bands reported in the enhancement measurements are the C=C stretch of the xanthene skeleton at 1650 cm^{-1} for R6G and 1590 cm^{-1} for BF. Other bands show similar enhancements. The intensity of the RRS varies rapidly with excitation wavelength as shown in Fig. 4, which is the excitation profile for low coverages of R6G on a silver-island film, along with the absorption spectrum of the film. There are two major contributions to the frequency dependence: The variation of the electromagnetic enhancement due to the silver islands, and the variation due to the molecular resonance. However, since the coverage is low enough, the absorption spectrum is essentially unchanged from that of the uncoated, or *p*-nitrobenzoate-covered films. Therefore, we expect that the spectral dependence of the electromagnetic enhancement, which is determined by the absorption, will be roughly the same as that of nonresonant RS from *p*-nitrobenzoate, which is also shown in Fig. 4. Our experiments are performed using 488 nm excitation, which is very near the peak electromagnetic contribution, yet causes the frequency of the RRS to be well removed from the peak of the fluorescence. The RRS is readily observable above the fluorescence on the island films. However, on the silica the intensity of the RRS is very low compared to the fluorescence, increasing the uncertainty in the enhancement measurement. The measured enhancements are $\sim 1\times10^{3}$ for both BF and R6G.

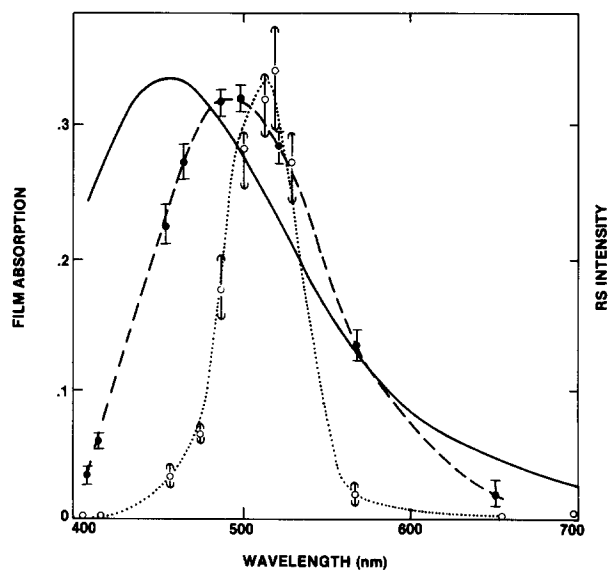

FIG. 4. Island-film excitation spectra of normal RS from *p*-nitrobenzoate (solid dots, dashed line) and RRS from R6G (circles, dotted line), compared to the absorption spectrum of the film (solid line).

We have also made enhancement measurements for higher coverages, where both the absorption spectrum and the excitation spectrum are radically different from those shown in Fig. 4. Since the local dielectric properties in the adsorbed layer are vastly altered compared to the case of low coverage or of *p*-nitrobenzoate coverage, the relative contribution to the total enhancement of the electromagnetic resonance compared to that of the molecular resonance cannot be determined experimentally. Again using 488 nm excitation, we have measured the enhancement of RRS for thick layers of the R6G and BF produced by dipping substrates in 10^{-3} M solutions. For these samples, the absorption and excitation profiles show complex, split peak behavior.[10] The enhancement levels for RRS are ~180 for R6G and ~170 for BF. Although the full spectral and coverage dependence of the enhancement for RRS has not been obtained, the trend is clear. The enhancement of RRS due to the silver is typically $\sim 1\times10^3$ at lower coverages and is substantially lower than normal RS. As the coverage increases, the enhancement of RRS decreases still further.

C. Fluorescence

For the measurements of the enhancement of fluorescence, an additional parameter must also be considered: the quantum efficiency (QE) of the fluorescence of the molecule in an electromagnetically inert environment. For this reason, we have used the two dye molecules R6G and BF. For dilute concentrations in solution, both have optical absorptions with roughly equal oscillator strengths and similar wavelength dependences. However, R6G has a QE of very nearly unity while that of BF is extremely low. At low coverages on a silica surface, the QE of R6G remains very high, while at higher coverages, dimer formation or other concentration-dependent effects cause quenching of the fluorescence and decrease the QE. In contrast, it is generally believed that BF has a lower QE in solution because of the increased vibrational and rotational degrees available to it compared to R6G.[25] This increases the nonradiative decay rate $\Gamma_0^{(NR)}$ while the radiative decay rate $\Gamma_0^{(R)}$ is thought to be roughly the same as that of R6G. Some of the extra intramolecular orientational degrees of freedom may be lost when the molecule is placed on a surface, causing the QE to rise. Nevertheless, it remains quite low, and from comparisons of the signals from approximately equal coverages of R6G and BF on bare silica, we estimate a surface QE for BF of ~0.01, suggesting that $\Gamma_0^{(NR)} \approx 100\,\Gamma_0^{(R)}$. All the enhancement measurements are again performed at low coverage so as to maintain the high QE of R6G as well as to ensure that the island film resonance, as measured by the absorption, is not changed from that of an uncoated island film. The excitation wavelength used is 458 nm, which is near the peak of both the molecular absorption band and the silver-island film electronic plasma resonance. As for the RRS, these enhancement measurements are made by comparing the signal from an island film to that from a bare silica substrate coated under identical dipping conditions.

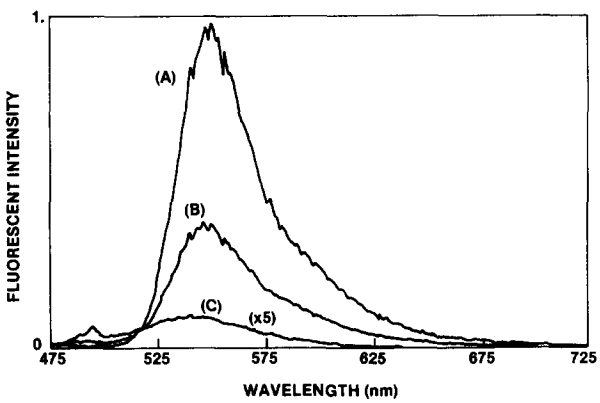

FIG. 5. Fluorescence spectra of R6G excited at 458 nm on (A) silica, (B) silver-island film on silica, and (C) silver-island film on aluminum.

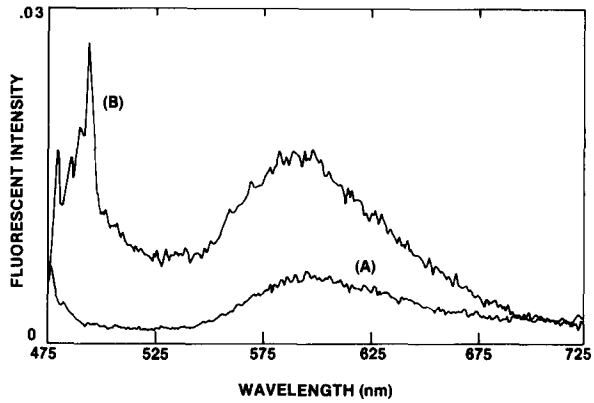

FIG. 6. Fluorescence spectra of BF excited at 458 nm on (A) silica and (B) silver-island film on silica. The spectra are normalized to the peak intensity of R6G on silica (see Fig. 5).

As shown in Fig. 5(A), the fluorescent emission from a low coverage of R6G on silica is quite intense. However, the emission from a coating of identical thickness on a silver-island film is reduced by a factor ~0.39 as shown in Fig. 5(B). In contrast, the emission from a thin layer of BF on silica is extremely weak, but is increased by a factor ~3.1 when the same thickness is applied on an island film, as shown in Figs. 6(A) and 6(B), respectively. Similar results are obtained with 488 nm excitation. We note further that the RRS of the dye molecules is observable from the silver-island films, unlike from the silica.

Since the emission of the R6G is so intense on the bare silica, a sizable amount of the total signal observed from the silver-island film arises from the molecules adsorbed directly on the silica, between the islands where the interaction with the silver is reduced. To obtain some idea of the relative contribution of those molecules directly on the silver to the total fluorescent signal, the experiments are repeated using a different type of substrate. A thick coating of aluminum is first put on the silica, thermally oxidized, and then covered with the silver islands. The bare aluminum effectively quenches the fluorescence of a dye coating, while the resonance of the silver islands still remains, as determined by reflectivity measurements. The Al

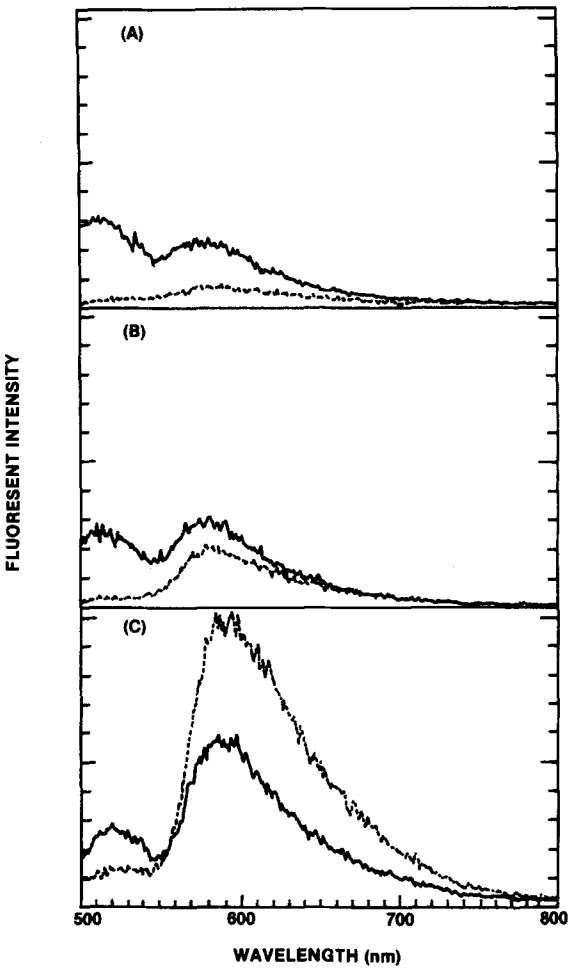

FIG. 7. Fluorescence spectra of BF excited at 458 nm on silica (dashed line) and silver-island film (solid line) at (A) room temperature and atmospheric pressure, (B) room temperature and 10 μm pressure, and (C) 14 K and in vacuum. All intensities normalized to the peak in (C).

film quenches the fluorescence from the molecules between the islands ensuring that any fluorescence observed originates from molecules adsorbed directly on the silver islands. As shown in Fig. 5(C), the fluorescence from the R6G is decreased still further on the island films on aluminum to ~0.02 of that observed on the bare silica. This tends to confirm that a substantial contribution to the signal from R6G on the island film on silica originates from those molecules between the islands, and shows that the effect of the silver islands is to quench the fluorescence of a high QE molecule.

As a further, direct confirmation of the dependence of the enhancement of fluorescence on the QE of the free molecule, the emission from BF on both an island film and bare silica is studied as a function of temperature and O_2 partial pressure above the sample. Decreasing the temperature and the number of O_2 molecules which can collide with excited dye molecules decreases the nonradiative decay rate, increasing the QE. This allows us to vary the QE of the same molecules in the same electromagnetic environment without any other changes. At room temperature and pressure the emission from the BF on the silica is very low, and there is substantial enhancement on the island film, as shown in Fig. 7(A). At room temperature and ~10 μm total pressure, the QE of the BF is increased, as evidenced by the larger emission from the silica, shown in Fig. 7(B). However, the emission from the island film is essentially unchanged, so the enhancement decreases to roughly unity. When the temperature is lowered to ~14 K, the QE, and hence the signal from the silica, is increased even further, as shown in Fig. 7(C). However, the signal from the island film is again increased only slightly, so the end result is now a decrease in the fluorescence signal due to the silver islands. This is direct confirmation of the decrease in the enhancement as the QE of the free molecule increases.

We emphasize here that we have experimentally established the dependence of the degree of enhancement on the QE of the adsorbed molecule by a considered choice of the adsorbate as well as careful control of the deposition conditions and technique. This ensures that the QE of the adsorbate on the inert silica surface is roughly the same as that in solution, with the variation due solely to the natural changes of the QE of the molecules themselves. This is in contrast to other work that has reported an enhancement for the fluorescence for R6G. In these cases, either a thick coating,[15] or a chemically adsorbed (and presumably modified) layer[16] was used. In separate experiments, we have verified that in each of these cases the QE of the adsorbate on the silica surface is substantially reduced from that in solution, resulting in an increased enhancement due to the rough silver. This illustrates the importance of the control of the QE of the adsorbate on an inert surface in making these quantitative measurements.

D. Spectroscopic implications

The results presented in the preceding sections establish an unambiguous hierarchy of enhancements for the various molecular inelastic optical scattering processes. Normal RS is enhanced by the silver-island film the most, with a typical value of ~10^5/molecule. The enhancement for RRS is much more dependent on the excitation wavelength and coverage. However, although the total signal per molecule is larger, the enhancement due to the silver islands is substantially reduced, with 10^3 a typical value for low coverage and 10^2 a typical value for thicker coverages. Fluorescence is enhanced even less, and the amount of increase depends strongly on the QE of the free molecule. A typical value of enhancement for a low QE molecule is ~10, while for a free QE of near unity, the fluorescence signal is actually decreased by about an order of magnitude. Besides the advantages of the enhancement istelf, this hierachy also has obvious importance for spectroscopic applications. In particular, the increased QE of fluorescence may be useful in fluorescence spectroscopy of molecules with very low QE. Similarly, the enhancement of RRS combined with the decrease in the fluorescence for molecules with high QE may simplify the spectroscopic use of RRS which would otherwise be obscured by the fluorescence. This may have particular importance in

the study of dye molecules, or those with biological significance.

An example of the potential power of this technique is shown in Fig. 8, which shows the RRS spectrum of BF. The solution spectrum is shown in Fig. 8(A), for 10^{-3} M in ethanol excited at 458 nm. The remaining spectra are for an island film dipped in this solution and excited at 458 nm in Fig. 8(B) and 515 nm in Fig. 8(C). We note that the solution spectrum and the island-film spectrum are essentially identical, both in the bands that appear and in their relative intensity. This appears to be a general feature of molecules that are physisorbed to the island films. We also note that the spectra do not change when the excitation wavelength is varied. We have found this to be the case for all exciting wavelengths, both for the solution and the island film RRS spectra. This remains the case even when an etalon is added to the laser to operate on a single mode. In contrast, a typical feature of RRS spectra of simple molecules is a variation of the spectra with excitation wavelength.[26] Finally, we note that the relative intensity of the RRS on the island films is comparable to the fluorescence. Spectra of similar quality can be readily obtained at all excitation wavelengths both from BF and R6G. In contrast, we are unable to obtain solution RRS spectra from BF when longer excitation wavelengths are used because of the intense fluorescence background.

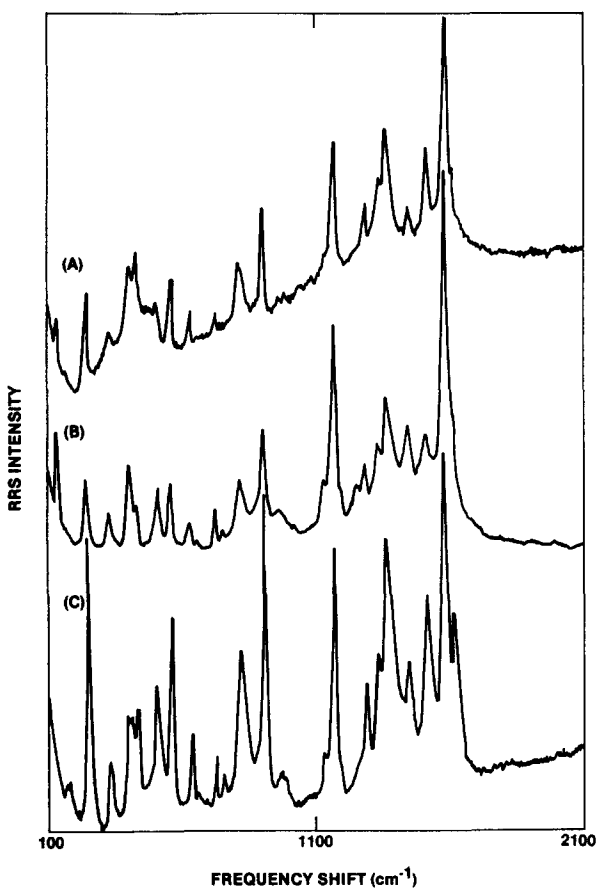

FIG. 8. RRS spectra of BF. (A) 10^{-3} M solution in ethanol, 458 nm excitation, (B) island film, 458 nm excitation, and (C) island film, 515 nm excitation.

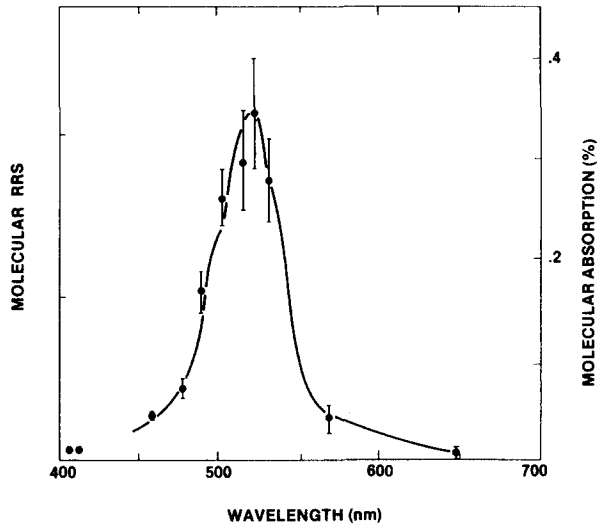

FIG. 9. Molecular contribution to RRS of R6G on a silver-island film (dots) and molecular absorption (solid line) of similar coverage on silica. Molecular RRS data normalized to absorption peak.

The problem is even more severe, and occurs at all excitation wavelengths for R6G, where the QE in solution is higher. These spectra demonstrate the potential usefulness of island films for spectroscopic purposes.

The relative enhancement of the RRS compared to the fluorescence also allows us to measure the excitation profile of RRS from R6G on an island film, shown in Fig. 4. Some additional important spectroscopic information can be readily obtained from these excitation profiles. Since the absorption spectra of the *p*-nitrobenzoate and R6G-coated films are identical, the spectral dependence of the electromagnetic contribution to the enhancement should also be similar, assuming that any effects due to variations in orientation or position play only a minor role in the excitation spectra. The electromagnetic contribution to the enhancement can then be determined directly from the nonresonant RS. The remaining contribution to the RRS intensity from the R6G arises from the molecular resonance itself. The wavelength dependence of this contribution can therefore be determined simply by taking the ratio of the RRS intensity from R6G to the normal RS intensity from *p*-nitrobenzoate, and is shown in Fig. 9. Since this contribution is solely from the molecular resonance, it represents an estimate of the excitation profile of RRS for a free R6G molecule. For comparison, we also show the absorption profile of an equivalent thickness of R6G on a bare silica disk, obtained using a high resolution spectrometer.[27] We note that the RRS excitation profile matches the absorption spectrum very closely for R6G. These results are obtained relatively easily using the island films, but would be extremely difficult to obtain by other techniques, again showing the potential usefulness of the relative enhancement ratios.

IV. THEORY

A. Free molecule

We now develop a physical model that treats all the inelastic light scattering processes in a unified way, and

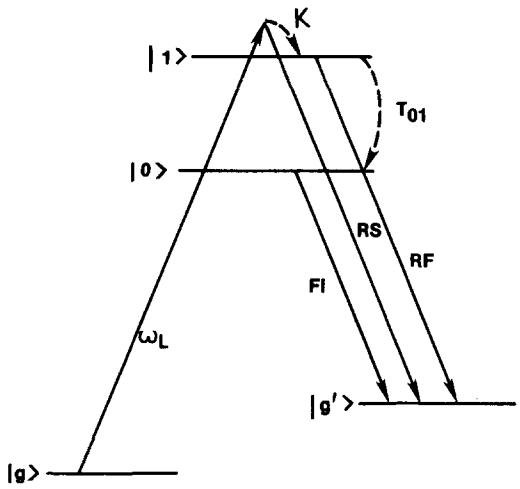

FIG. 10. Energy levels and scattering processes for four-level model. Dashed lines represent nonradiative processes and solid lines represent radiative transitions.

can account for the hierarchy of enhancements that are observed. Our approach is to first develop a simple picture of the inelastic scattering processes from a molecule in an electromagnetically inert environment. Scattering intensities are expressed in terms of excitation rates and emission yields, which allow a physical interpretation of the effects that occur upon extension to the case of the molecule near a silver island. The validity of this approach to the scattering from a free molecule is confirmed more rigorously in the following section, using the density matrix formalism to treat the light scattering processes. Finally, we use the isolated spheroid model to extend the results to include the surface-induced effects, and develop expressions for the enhancement ratios of each light scattering process.

We start by considering the light scattering from a molecule idealized as the four-level system shown in Fig. 10. State $|g\rangle$ denotes the initial vibronic state associated with the ground state electronic manifold, states $|0\rangle$ and $|1\rangle$ are vibronic states associated with the excited electronic manifold, and state $|g'\rangle$ is an excited vibronic state of the ground state electronic manifold. Four light scattering processes will be considered: normal RS, RRS, resonance fluorescence (RF), and (relaxed) fluorescence. These processes are depicted schematically in Fig. 10. Raman scattering is a coherent light scattering process, which involves the virtual scattering of a photon from state $|1\rangle$. The frequency mismatch between the energy level difference of state $|1\rangle$ and $|g\rangle$ and the laser frequency ω_L is denoted by $\Delta\omega = \omega_L - \omega_1 + \omega_g$. For large $\Delta\omega$, the scattering process is normal RS, while for small $\Delta\omega$, the scattering becomes RRS. In contrast to RS, fluorescence is defined as an incoherent light scattering process following dephasing interactions with a thermal environment. Resonance fluorescence follows a "pure" dephasing (proper T_2 process) which causes a real absorption in state $|1\rangle$ followed by a radiative decay to state $|g'\rangle$. Relaxed fluorescence involves an absorption to state $|1\rangle$ followed by a thermal population relaxation to state $|0\rangle$ and finally an emission to state $|g'\rangle$. In our cw experiments, where the phase and temporal relationship between the incident and scattered radiation is not determined, we do not distinguish between RRS and RF. Rather the RRS we measure corresponds to the sum of what we have theoretically defined as RRS and RF.

We begin by writing an expression for the absorption cross section for making a transition to state $|1\rangle$ from state $|g\rangle$, $(h=1)$,

$$\sigma_a = \frac{\mu^2}{c}\,\chi_{1g}\gamma_1\,\frac{1}{(\Delta\omega)^2+\left(\frac{\gamma_1}{2}\right)^2}\ ; \tag{1}$$

here μ is the electronic transition moment connecting the ground and excited electronic states and χ_{1g} is the appropriate Franck–Condon factor. The full width of the state $|1\rangle$ is denoted by γ_1. It includes both an irreversible population relaxation contribution Γ_1, a pure dephasing contribution κ, and a thermalization rate from state $|1\rangle$ to state $|0\rangle$ T_{01},

$$\gamma_1 = \Gamma_1 + \kappa_1 + T_{01}\ . \tag{2}$$

We assume an energy separation between states $|1\rangle$ and $|0\rangle$ much larger than $k_B T$, where k_B is the Boltzman constant and T is the temperature. Thus, we neglect repopulation of state $|1\rangle$ by thermal transfer from state $|0\rangle$. The population relaxation rate can also be split into radiative and nonradiative components

$$\Gamma_1 = \Gamma_1^{(R)} + \Gamma_1^{(NR)}\ , \tag{3}$$

where $\Gamma_1^{(NR)}$ is the sum of the rates of all remaining nonradiative decay processes from state $|1\rangle$ and $\Gamma_1^{(R)}$ is the radiative decay rate from $|1\rangle$ to $|g'\rangle$. The absorption rate can now be written as

$$\Omega = \sigma_a |E_L|^2\ , \tag{4}$$

where E_L is the local electric field at the molecule due to the laser.

The integrated radiative emission rate from an excited state $|i\rangle$ to state $|g'\rangle$ may likewise be written as

$$\Gamma_i^{(R)} = 2\pi\mu^2\chi_{ig'}\rho_{ig'}\ , \quad (i=0,1)\ , \tag{5}$$

where $\rho_{ig'}$, is the density of final photon states. The emission yield Y_{em} for any light scattering process can then be defined as the ratio of the radiative decay rate to the total of all decay rates available to state $|i\rangle$. Finally, we define a transfer yield Y_{trans}, which expresses the probability of some dephasing event occuring before light emission in a coherent scattering process. Thus, for RF it represents the probability of a pure dephasing event, while for fluorescence it represents the probability of a thermal decay from state $|1\rangle$ to state $|0\rangle$. For RS, which is a coherent process, the transfer yield is taken as unity. We can now express the scattering intensity for each process in terms of an excitation rate, an emission yield, and a transfer yield

$$I = Y_{em}Y_{trans}\Omega\ . \tag{6}$$

We first consider RS, and write the emission yield as the ratio of the radiative emission rate to the total decay rate of state $|1\rangle$,

$$(Y_{em})_{RS} = \frac{\Gamma_1^{(R)}}{\gamma_1} \quad . \tag{7}$$

Thus, the scattering intensity for RS is

$$I_{RS} = \frac{\Gamma_1^{(R)}}{\gamma_1} \sigma_a |E_L|^2 \quad . \tag{8}$$

We note that formally the γ_1 in the denominator cancels the term γ_1 in the numerator of σ_a so that the resulting expression

$$I_{RS} = \frac{2\pi}{c} \frac{\mu^4 \chi_{1g} \chi_{1g'} \rho_{gg'}}{(\Delta\omega)^2 + (\gamma_1/2)^2} |E_L|^2 \tag{9}$$

is the same as that obtained using second order perturbation theory for the RRS cross section. Furthermore, for our model, we consider I_{RS} to be the scattering intensity for RRS for $\Delta\omega \lesssim \gamma_1$, and the scattering intensity for normal RS $\Delta\omega \gg \gamma_1$.

Next we consider RF, which is an incoherent process wherein a pure dephasing event occurs causing a real absorption in state $|1\rangle$. The transfer yield reflects the probability of this dephasing occurring

$$(Y_{trans})_{RF} = \frac{\kappa_1}{\gamma_1} \quad . \tag{10}$$

Since dephasing has already occurred, the emission yield involves all the decay rates of the dephased population of state $|1\rangle$, and is

$$(Y_{em})_{RF} = \frac{\Gamma_1^{(R)}}{\Gamma_1 + T_{01}} \quad . \tag{11}$$

Thus, the scattering intensity for resonance fluorescence is

$$I_{RF} = \frac{\Gamma_1^{(R)}}{\Gamma_1 + T_{01}} \frac{\kappa_1}{\gamma_1} \sigma_a |E_L|^2 \quad . \tag{12}$$

The emission frequency of the RF as we have defined it is identical to that of RRS when $\Delta\omega$ is very small. Since we do not experimentally distinguish the two scattering processes, we can formally add the expression for their scattering intensities and obtain what we will label as the RRS intensity

$$I_{RRS} = \frac{\Gamma_1^{(R)}}{\Gamma_1 + T_{01}} \sigma_a |E_L|^2 \quad . \tag{13}$$

In this expression, the emission yield is the probability of radiative emission for the total population decay from state $|1\rangle$.

Finally, we consider relaxed fluorescence, which consists of an absorption followed by a population transfer and finally an emission process. The population transfer event provides a phase interruption and causes a real transition to state $|1\rangle$ to occur. The transfer yield is thus the ratio of the rate for thermal decay from state $|1\rangle$ to state $|0\rangle$ relative to the sum of all rates of population decay from state $|1\rangle$,

$$(Y_{trans})_{F1} = \frac{T_{01}}{\Gamma_1 + T_{01}} \quad . \tag{14}$$

The emission yield is simply the radiative yield of state $|0\rangle$,

$$(Y_{em})_{F1} = \frac{\Gamma_0^{(R)}}{\Gamma_0} \quad , \tag{15}$$

where

$$\Gamma_0 = \Gamma_0^{(R)} + \Gamma_0^{(NR)} \quad . \tag{16}$$

Thus, the scattering intensity for fluorescence is

$$I_{F1} = \frac{\Gamma_0^{(R)}}{\Gamma_0} \frac{T_{01}}{\Gamma_1 + T_{01}} \sigma_a |E_L|^2 \quad . \tag{17}$$

Equations (8), (12), and (17) form the desired expressions for the intensity of inelastic light scattering for the processes under consideration.

The four level model used here is a convenient but grossly oversimplified approximation of the actual molecular system. With the large dye molecules used in our experiments, the excited (intermediate) state manifold involves a very large number of levels. Part of these levels are excited due to transitions from thermally populated vibrational levels in the ground electronic state. Even with such hot-line excitations disregarded, there will be many intermediate levels excited due to the large density of states. The excited states (in particular level $|1\rangle$) therefore represent groups of closely lying levels, and the vibrational relaxation and dephasing processes introduced in the four-level model correspond to rather complicated multilevel relaxation processes. In particular, the dephasing rate for the intermediate levels is affected not only by the pure dephasing interaction between the molecule and its environment, but also includes thermal transitions between closely lying molecular levels, as well as intramolecular vibrational relaxation. We note in passing that the existence of many intermediate levels is probably the reason why excitation into different spectral regions gives rise to the same RRS spectrum (see Fig. 8). With many intermediate levels involved, many Franck–Condon factors are sampled by the transition process, and the resulting averaged Franck–Condon factor is no longer very sensitive to the incident energy, in sharp contrast to the small-molecule case.[26] Furthermore, the similarity between the molecular RRS excitation profile and the molecular absorption profile for R6G, shown in Fig. 9, also implies that there cannot be a strong frequency dependence to the Franck–Condon factors. This lends additional support to the interpretation of the Franck–Condon factors as representing average values over the large number of energy levels involved.

The four-level model is still useful under these circumstances for the following reasons: (a) the observed intensities arise from superpositions of many intermediate levels, each subjected to the basic processes introduced in the four-level model, namely dephasing and population relaxation; (b) even though the microscopic details of the dephasing and population relaxation are different in a system with a dense level structure compared with a sparse level system, these differences will enter mainly when one attempts to carry out a microscopic calculation of the dephasing and relaxation rates. In the present work we avoid this complicated task by introducing these rates as phenomenological parameters.

B. Density matrix formulation

Before extending the theoretical expressions for the scattering intensities to include the effects of a rough surface, we verify the results, which we have obtained from heuristic arguments in the last section, by providing a more rigorous derivation of the intensities using the density matrix formalism. We use the same four-level model depicted in Fig. 10. This model has been used previously to account for light scattering from large molecules,[28] but in contrast to that work, here we introduce the thermal relaxation processes in a phenomenological way. This avoids many of the complications and makes it possible to arrive at the results in a considerably more transparent way.

We start with the Hamiltonian for our system,

$$H = H_m + H_R + V + \text{(intramolecular damping and thermal interactions)} . \tag{18}$$

H_m is the molecular Hamiltonian, H_R is the Hamiltonian for the radiation field, and V is the molecule–radiation field interaction. The terms which are not written explicitly include thermal interactions with the surroundings leading to dephasing and thermal relaxation as well as interactions with other molecular states, not included in our model, leading to intramolecular radiationless transitions.

In the limit of low incident intensity, where nonlinear optical processes may be disregarded, the relevant eigenstates of $H_0 = H_m = H_R$ are

$$\begin{aligned} &|i\rangle = |g, k\rangle; \quad E_i \equiv \omega_i = (\omega_g + \omega_L) , \\ &|f\rangle = |g', k'\rangle ; \quad E_f \equiv \omega_f = (\omega_{g'} + \omega') , \\ &|0\rangle = |0, 0\rangle ; \quad E_0 \equiv \omega_0 , \quad |1\rangle = |1, 0\rangle ; \quad E_1 \equiv \omega_1 , \end{aligned} \tag{19}$$

where k denotes the state of the incident photon of frequency ω_L, and k' the state of the final (scattered or emitted) photon of frequency ω'. The states $|0, 0\rangle$ and $|1, 0\rangle$ describe the molecules in the $|0\rangle$ or $|1\rangle$ excited states with no photons. Keeping only terms to fourth order in V and those which describe the optical processes pictured in Fig. 10, Eq. (18) may be written in the form

$$\begin{aligned} H = {} & \omega_i |i\rangle\langle i| + \omega_f |f\rangle\langle f| + \omega_0 |0\rangle\langle 0| + \omega_1 |1\rangle\langle 1| \\ & + \{V_{i1} |i\rangle\langle 1| + V_{1i} |1\rangle\langle i1|\} + \{V_{1f} |1\rangle\langle f| + V_{f1} |f\rangle\langle 1|\} \\ & + \{V_{0f} |0\rangle\langle f| + V_{f0} |f\rangle\langle 0|\} \\ & + \text{intramolecular damping and thermal interactions.} \end{aligned} \tag{20}$$

In Eq. (20) we have neglected the radiative coupling between $|g\rangle$ and $|0\rangle$ since we are interested in the resonant $|g\rangle \rightarrow |1\rangle$ excitation and in processes which lead to the final state $|g'\rangle$.

Next we consider the equations of motion for the matrix elements of the density operator ρ,

$$\dot{\rho}_{ab} = -i[H, \rho]_{ab} . \tag{21}$$

In writing these equations we keep only such terms that lead to a description of the process to the lowest (fourth) order in V. We obtain

$$\dot{\rho}_{ii} = -2\mathrm{Im}(V_{1i}\rho_{i1}) , \tag{22a}$$

$$\dot{\rho}_{ff} = -2\mathrm{Im}(V_{1f}\rho_{f1}) + (V_{0f}\rho_{f0}) , \tag{22b}$$

$$\dot{\rho}_{00} = -T_{10}\rho_{00} + T_{01}\rho_{11} - \Gamma_0\rho_{00} , \tag{22c}$$

$$\dot{\rho}_{11} = -2\,\mathrm{Im}(V_{i1}\rho_{1i}) - T_{01}\rho_{11} + T_{10}\rho_{00} - \Gamma_1\rho_{11} , \tag{22d}$$

$$\dot{\rho}_{if} = -i\omega_{if}\rho_{if} + iV_{if}\rho_{i1} - (1/2)\eta\rho_{if} , \tag{22e}$$

$$\dot{\rho}_{i1} = -i\omega_{i1}\rho_{i1} + iV_{i1}\rho_{ii} - (1/2)\gamma_1\rho_{i1} , \tag{22f}$$

$$\dot{\rho}_{f1} = -i\omega_{f1}\rho_{f1} - iV_{f1}\rho_{11} + iV_{i1}\rho_{fi} - (1/2)\gamma_1\rho_{f1} , \tag{22g}$$

$$\dot{\rho}_{f0} = -i\omega_{f0}\rho_{f0} - iV_{f0}\rho_{00} - (1/2)\gamma_0\rho_{f0} , \tag{22h}$$

with $\rho_{ab} = \rho_{ba}^*$ and $\omega_{ab} = \omega_a - \omega_b$. The terms involving the damping and thermal relaxation rates T, Γ, γ, and η are added phenomenologically. As discussed previously, T_{01} and T_{10} are the thermal transition rates from $|1\rangle$ to $|0\rangle$ and from $|0\rangle$ to $|1\rangle$, respectively [$T_{10}/T_{01} = \exp(-\omega_{10}/k_B T)$]. Γ_0 and Γ_1 are the population relaxation rates associated with levels $|0\rangle$ and $|1\rangle$. γ_0 and γ_1 are the total widths associated with levels $|0\rangle$ and $|1\rangle$ and include dephasing widths in addition to population relaxation rates. We assume for simplicity that relaxation in the ground electronic levels $|g\rangle$ and $|g'\rangle$ may be disregarded. Accordingly, no damping terms appear in the equations for $\dot{\rho}_{ii}$ and $\dot{\rho}_{ff}$ and η will be put to 0 at the end of the calculation.

We are interested in the steady state solution for $\dot{\rho}_{ff}$ (rate of formation of the final photon state with $\dot{\rho}_{00} = \dot{\rho}_{11} = \dot{\rho}_{if} = \dot{\rho}_{f1} = \dot{\rho}_{f0} = 0$). The result (after taking the limit $\eta \rightarrow 0$) is

$$\frac{\dot{\rho}_{ff}}{\dot{\rho}_{ii}} = \frac{2\pi}{c}\,\frac{|V_{i1}V_{1f}|^2}{\omega_{i1}^2 + (\gamma_1/2)^2} \times \left\{ \delta(\omega_{fi}) + \frac{\kappa_1}{\tilde{\Gamma}_1}\,\frac{\gamma_1/2\pi}{\omega_{f1}^2 + (\gamma_1/2)^2} + \left|\frac{V_{f0}}{V_{f1}}\right|^2 \frac{T_{01}}{T_{10}+\Gamma_0}\,\frac{\gamma_1}{\tilde{\Gamma}_1}\,\frac{\gamma_0/2\pi}{\omega_{f0}^2 + (\gamma_0/2)^2} \right\} , \tag{23}$$

where

$$\tilde{\Gamma}_1 = \Gamma_1 + T_{01} - \frac{T_{01}T_{10}}{T_{10}+\Gamma_0} \tag{24}$$

and where the dephasing rate is

$$\kappa_1 = \gamma_1 - \tilde{\Gamma}_1 . \tag{25}$$

$\tilde{\Gamma}_1$ in Eq. (24) may be interpreted as the total *irreversible* population relaxation rate of level $|1\rangle$ (note that T_{01} is multiplied by the probability not to have back transfer from $|0\rangle$ to $|1\rangle$). This equation is slightly more general than Eq. (2) because repopulation from state $|0\rangle$ to state $|1\rangle$ is now considered. κ_1 in Eq. (25) may be rewritten as

$$\kappa_1 = \gamma_1 - \Gamma_1 - T_{01} + \frac{T_{01}T_{10}}{T_{10}+\Gamma_0} . \tag{26}$$

The first three terms on the right-hand side correspond to pure dephasing of level $|1\rangle$ while the last term is the contribution to the dephasing rate from the thermal repopulation process $|1\rangle \rightarrow |0\rangle \rightarrow |1\rangle$.

The result [Eq. (23)] has been obtained previously,[28] but is in a simpler form here because we have neglected the effects of interference between levels $|0\rangle$ and $|1\rangle$. Such effects were disregarded here by taking diagonal damping matrices. The scattering intensity is seen to

follow the absorption line shape $[\omega_{i1}^2+(\gamma_1/2)^2]^{-1}$, and is characterized by three emission peaks: The RS peak at $\omega_f=\omega_i$, the RF peak at $\omega_f=\omega_1$ and the regular (relaxed) fluorescence peak at $\omega_f=\omega_0$. To get the total (integrated) intensity associated with these emission components, we have to sum each over all the final photon states. To this end we multiply Eq. (23) by $\rho(\omega')$ and integrate over ω'. We further note that in the Condon approximation the radiative coupling matrix elements are

$$|V_{i1}|^2=\mu^2\chi_{1g}\ ,\quad |V_{f1}|^2=\mu^2\chi_{1g'}\ ,\quad |V_{f0}|^2=\mu^2\chi_{0g'}\ , \tag{27}$$

where μ is the transition dipole element between the ground and excited electronic states while χ_{1g}, $\chi_{1g'}$, and $\chi_{0g'}$ are the Franck–Condon factors associated with the particular vibrational levels. Denoting also

$$\omega_{i1}=\omega_L-\omega_1-\omega_g\equiv\Delta\omega\ ,$$

we obtain

$$I_{\rm RS}=\frac{2\pi}{c}\ \frac{\mu^4\chi_{1g}\chi_{1g'}\rho_{ig'}}{(\Delta\omega)^2+\left(\frac{\gamma_1}{2}\right)^2}\ |E_L|^2\ , \tag{28}$$

$$I_{\rm RF}=\frac{2\pi}{c}\ \frac{\mu^4\chi_{1g}\chi_{1g'}\rho_{1g'}}{(\Delta\omega^2)+\left(\frac{\gamma_1}{2}\right)^2}\ \frac{\kappa_1}{\tilde{\Gamma}_1}\ |E_L|^2\ , \tag{29}$$

$$I_{\rm F1}=\frac{2\pi}{c}\ \frac{\mu^4\chi_{1g}\chi_{0g'}\rho_{0g'}}{(\Delta\omega)^2+\left(\frac{\gamma_1}{2}\right)^2}\ \frac{T_{01}}{T_{10}+\Gamma_0}\ \frac{\gamma_1}{\tilde{\Gamma}_1}\ |E_L|^2\ . \tag{30}$$

Identifying the absorption cross section σ_a [Eq. (1)] and the radiative emission rates from $|1\rangle$ and $|0\rangle$, Γ_1, and Γ_0, respectively [Eq. (5)], and including the applied laser field $|E_L|^2$ these equations become identical to Eqs. (8), (12), and (17) derived phenomenologically in the previous section if the energy spacing between levels $|1\rangle$ and $|0\rangle$ is much greater than k_BT.

C. Surface-induced effects

We now generalize the expressions for the intensity of the light scattering processes to include the presence of silver islands. We do this initially within the context of a single molecule near an isolated dielectric spheroid.[2,12] The isolated dielectric spheriod model has been successful in providing qualitative and, in some cases, quantitative interpretations of many observations of the electromagnetic interactions which occur near rough surfaces. Our expressions for the free molecule are ideally suited to this sort of generalization. The results thus obtained will provide a guide to the extension to the case of island films when the theory is compared with our experimental results in the following section.

There are three major effects that the electronic plasma resonances in the silver islands have on the molecular light scattering processes. First, the strengths of the local excitation fields are increased by the morphology and dielectric properties of the islands through the excitation of electronic plasma resonances. We denote this field amplification factor by $A(\omega_L)$. The increased local field intensity results in an enhanced absorption rate which is reflected by replacing $|E_L|^2$ by $|A(\omega_L)|^2|E_L|^2$. The second effect of the silver islands occurs in the emission process. The molecular emission dipole will induce a macroscopic polarization in the islands which will become large near the frequency of the electronic plasma resonance. The in-phase dipolar component of this response will increase the total emission dipole resulting in a concomitant increase in the radiative emission rate.[12] This electromagnetic interaction reflects the coupling of a molecular dipole to the macroscopic dipole in the island and then to the emitted radiation field. Thus, in analogy to the enhanced local exciting field, the enhancement factor is again given by $A(\omega')$, but evaluated at the emission frequency ω'. This enhancement is reflected by an increased radiative emission rate near the surface, requiring the replacement of $\Gamma_i^{(R)}$ by $|A(\omega')|^2\Gamma_i^{(R)}$ (Ref. 12). Finally, any molecular excited state will also have an additional nonradiative decay channel when the molecule is near the surface. This damping arises from the out-of-phase dipolar component of the induced macroscopic polarization in the island, as well as from the higher order, nonradiating poles induced because the island is in the near field of the molecular dipole. Alternatively, we may view the damping as arising from the nonradiative branch of the decay of the electronic plasma resonance induced in the island by the molecular dipole. Thus, the presence of the rough surface results in an additional population decay rate for each excited state

$$\Gamma_i^{(S)}=\Gamma_i^{(S,NR)}+\Gamma_i^{(S,R)}\ . \tag{31}$$

The existence of this increased decay rate has been observed directly in measurements of the fluorescent lifetime of europium ions on silver-island films.[18]

We can now express the absorption rate, transfer yields, and emission yields for each light scattering process for a molecule near a spheroid. We assume that the purely molecular parameters, including the Franck–Condon factors, the electronic transition matrix elements, and the dephasing and thermalization rates, are unchanged by the presence of the surface. While this is perhaps somewhat of an oversimplification, it seems reasonable in light of the similarity between the fluorescence, RS and RRS spectra of the molecules on the silver-island films, on the silica surface, or in a solvent. Thus, denoting the scattering intensities near a spheroid with an asterisk, we obtain

$$I_{\rm RS}^*=\frac{2\pi}{c}\ \frac{\mu^4\chi_{1g}\chi_{1g'}\rho_{1g'}}{(\Delta\omega)^2+\left(\frac{\gamma_1+\Gamma_1^{(S)}}{2}\right)^2}\ |A(\omega_L)|^2|A(\omega')|^2|E_L|^2\ , \tag{32}$$

$$I_{\rm RF}^*=\frac{2\pi}{c}\ \frac{\mu^4\chi_{1g}\chi_{1g'}\rho_{1g'}}{(\Delta\omega)^2+\left(\frac{\gamma_1+\Gamma_1^{(S)}}{2}\right)^2}\ \frac{\kappa_1}{\Gamma_1+T_{01}+\Gamma_1^{(S)}}\times|A(\omega_L)|^2|A(\omega')|^2|E_L|\ , \tag{33}$$

$$I_{\rm F1}^*=\frac{2\pi}{c}\ \frac{\mu^4\chi_{1g}\chi_{0g'}\rho_{0g'}}{(\Delta\omega)^2+\left(\frac{\gamma_1+\Gamma_1^{(S)}}{2}\right)^2}\ \frac{T_{01}}{\Gamma_0+\Gamma_0^{(S)}}\ \frac{\gamma_1+\Gamma_1^{(S)}}{\Gamma_1+T_{01}+\Gamma_1^{(S)}}\times|A(\omega_L)|^2|A(\omega')|^2|E_L|^2\ . \tag{34}$$

Since we ultimately wish to compare the calculated values with experiment, we compute the ratio of the

light scattering intensities of the surface-adsorbed molecule to those of the free molecule. In so doing, we also distinguish resonant from nonresonant properties by approximating $\Delta\omega \gg \gamma_1$ for nonresonant scattering and $\Delta\omega \ll \gamma_1$ for resonant scattering. Thus, we define the enhancement ratios for RS, RRS, ahd fluorescence as

$$R_{RS} = |A(\omega_L)|^2 |A(\omega')|^2 , \tag{35}$$

$$R_{RRS} = |A(\omega_L)|^2 |A(\omega')|^2 \frac{\gamma_1}{\gamma_1 + \Gamma_1^{(s)}} \frac{\Gamma_1 + T_{01}}{\Gamma_1 + T_{01} + \Gamma_1^{(s)}} , \tag{36}$$

$$R_{FI} = |A(\omega_L)|^2 |A(\omega')|^2 \frac{\gamma_1}{\gamma_1 + \Gamma_1^{(s)}} \frac{\Gamma_1 + T_{01}}{\Gamma_1 + T_{01} + \Gamma_1^{(s)}} \times \frac{\Gamma_0}{\Gamma_0 + \Gamma_0^{(s)}} . \tag{37}$$

We have included the RF intensity in the ratio for RRS.

V. DISCUSSION

We now compare the theoretical expressions for the enhancement ratios, developed in the preceding section, with our measurements on the island films. To do so, we begin by extending the theory developed for a single molecule near an isolated spheroid to treat the more realistic case of the island films. We show that this can be done in a straightforward fashion by using experimentally measured values of the average enhancement factors for a film rather than analytically calculated values for an isolated spheroid. We then proceed with a detailed comparison of the theory to the experiment. However, since experimentally measured values of the phenomenological molecular rates used in our four-level model have not, to our knowledge, been obtained, we are unable to calculate *a priori* the expected enhancement ratios. Instead, we use the experimentally determined enhancement ratios to obtain numerical estimates for the effects of the surface on these molecular rates. Each light scattering process contributes additional information, and taken as a whole, we are able to develop a consistency between all our measurements and the theory. This type of comparison is made possible by our measurement of the complete series of scattering processes, all on optically identical surfaces. In the concluding section, we discuss how the full range of optical scattering phenomena studied leads to a physical picture of the effects of the localized electronic plasma resonances on each portion of the optical scattering process from adsorbed molecules.

The expressions developed in the preceding section describe a single molecule near an isolated island. In fact, the electromagnetic interactions with the island are very strongly dependent on the exact position of the molecule, as both the field enhancement factor $A(\omega)$ and the surface-induced decay rate $\Gamma_i^{(s)}$ are functions of both position as well as the frequency. The strength of the electromagnetic interaction varies strongly around the surface of an island itself. In a backscattering geometry, the maximum increase in the optical field occurs at the edge of the island where the field is normal to the surface. Besides the variation for molecules at different positions on the surface of the silver island itself, there is an even stronger variation for the roughly half of the molecules adsorbed directly on the silica substrate between the islands. For the weaker intensity scattering from normal RS and RRS, these molecules can be expected to contribute very little to the total measured signal. However, this is not the case for fluorescence measurements, where, in cases of intense scattering, these molecules can even dominate the total signal from the island films. Furthermore, modeling an individual island as an isolated spheroid is inadequate for the films used in these experiments. The islands are separated by distances comparable to their size and the electromagnetic interactions between the islands play a significant role in their optical behavior, both shifting the resonance to a lower frequency as well as broadening it.[9]

In order to compare the theoretical expressions with our experimental results, we must account for both the spatial variations over the film as well as the effects of the electromagnetic interactions between the islands. This is readily accomplished by using the theoretical expression obtained from the isolated spheroid model as a guide to the spatial variations. Thus, we take $A(\omega)$ to represent some average value of the field enhancement around the surface of the islands, which includes the effects of both the spatial variations and the interactions between the islands. Similarly, $\Gamma^{(s)}$ is taken to represent an average value of the surface-induced decay rate for molecules on the silver. Instead of using the calculated[2,12] values of $A(\omega)$ and $\Gamma^{(s)}$, we will express these quantities in terms of experimentally measured parameters. This approach has been used successfully to account for the frequency dependence and the magnitude of the SERS on our island films as well as the behavior of the fluorescent lifetime of molecules adsorbed on the films. The field enhancement was expressed in terms of the measured absorption of the film,[10] while the increase in the total decay rate was measured directly.[18] Here, we concentrate on low adsorbate coverage in the case of absorbing molecules, so as to consider the effects of the electronic plasma resonance on the scattering process while avoiding the additional complications of changes in the plasma resonance induced by thicker absorbing coatings.

Using these generalized interpretations of $A(\omega)$ and $\Gamma^{(s)}$, we can now compare the theory to the experimental results. When the laser frequency is far from resonance, the effects of the molecular absorption are removed, and, as shown in Eq. (35), the enhancement ratio for normal RS reduces to the product of the average field intensity enhancements at the laser and emission frequencies, in agreement with earlier theoretical treatments of SERS.[2-5] The experimentally measured R_{RS} allows us to obtain a value for $|A(\omega_L)|^2 |A(\omega')|^2 \sim 10^5$. Because of the direct relationship between the enhancement and the absorption, this value remains unchanged if the absorption spectrum of the film is unchanged, and thus, can also be used in the other expressions for low coverage of dye molecules. Furthermore, near the frequency of the peak electromagnetic enhancement the variation with ω_L and ω' is relatively slow, so $|A(\omega_L)|^2 \sim |A(\omega')|^2$. Thus, the average field intensity is enhanced by ~300, which is consistent with the enhancement factor estimated from second harmonic genera-

tion measurements on electrochemically roughened surfaces.[29]

The situation is changed when $\Delta\omega$ becomes comparable to the width of the molecular state. In this case, the absorption is still enhanced by the field intensity enhancement $|A(\omega_L)|^2$ but this enhancement is mitigated by the increased width of the absorbing state, $|1\rangle$, due to the additional surface decay channel, represented by $\Gamma_1^{(s)}$. This has the effect of broadening the effective width of the molecular absorption resonance and, therefore, decreasing its magnitude. This decrease in the excitation rate is reflected in the term $\gamma_1/[\gamma_1+\Gamma_1^{(s)}]$ in both R_{RRS} and R_{F1}, Eqs. (36) and (37), respectively. In fact, as the molecular resonance becomes stronger, due to a decreased width γ_1 the enhancement of the excitation rate is reduced even further. The emission yield for RRS is also increased by the more rapid radiative emission rate, leading to the $|A(\omega')|^2$ term. However, this is again mitigated by the additional branching channels to the surface, resulting in the remaining ratio $(\Gamma_1+T_{01})/[\Gamma_1+T_{01}+\Gamma_1^{(s)}]$ in Eq. (36). Since each of the ratio terms in Eq. (36) is less than unity, R_{RRS} is predicted to be less than R_{RS}, in agreement with our measurements. This decrease arises from the additional damping caused by the coupling to the electronic plasma resonance which becomes important for small $\Delta\omega$, when the molecular damping plays a role in the scattering process. Using $R_{RRS}\sim 10^3$ as a typical experimental value, we can obtain a numerical estimate for the additional damping,

$$\frac{\Gamma_1+T_{01}}{\Gamma_1+T_{01}+\Gamma_1^{(s)}}\ \frac{\gamma_1}{\gamma_1+\Gamma_1^{(s)}}\approx 10^{-2}\ . \tag{38}$$

For a large molecule in a condensed phase at room temperature, it seems reasonable to take $\kappa_1 \leq T_{01}$, suggesting that $\gamma_1/(\gamma_1+\Gamma_1^{(s)})\sim 0.1$. This suggests that $\Gamma_1^{(s)}\sim 10\gamma_1$, so that the actual increase in the excitation rate in the dye molecules due to the presence of the silver islands is only a factor of ~30. We note that this is considerably less than would be predicted by considering the field enhancement alone.

For the thicker coverages of dye molecules the situation becomes considerably more complicated. However, a qualitative understanding of the results can be obtained by recognizing that a thick coating of dye is strongly absorbing and, therefore, damps the electronic plasma resonance of the silver. This has the effect of decreasing the field enhancement factors $A(\omega)$, further decreasing the enhancement of RRS, as is observed. In fact, qualitative agreement with the data has been obtained for both the spectral dependence of the absorption, and the enhancement of RRS, using a coated, isolated spheroid model.[30]

Next, we examine the results for fluorescence. As is the case for RRS, the excitation rate is increased due to the enhancement of the local pump field, but decreased due to the increased width of the absorbing state. In addition, the transfer yield is decreased because there is now the additional possible branching from state $|1\rangle$ to the silver islands. This results in the term $(\Gamma_1+T_{01})/(\Gamma_1+T_{01}+\Gamma_1^{(s)})$ in R_{F1}. Finally, the emission rate is increased by the response induced in the island, as reflected by the term $|A(\omega')|^2$. However, the effective yield is decreased by the additional possible decay to the surface as reflected in the term $\Gamma_0/(\Gamma_0+\Gamma_0^{(s)})$. The resultant yield must by investigated for the two limiting cases of high and low QE for free molecules.

We begin with R6G, whose QE is very high, so that $\Gamma_0\approx\Gamma_0^{(R)}\gg\Gamma_0^{(NR)}$. Since $\Gamma_0^{(s,R)}=|A(\omega')|^2\Gamma_0^{(R)}$ (Ref. 12), we can write the ratio of the effective emission yields as

$$\frac{\Gamma_0}{\Gamma_0+\Gamma_0^{(s)}}\approx\frac{\Gamma_0^{(R)}}{|A(\omega')|^2\Gamma_0^{(R)}+\Gamma_0^{(s,NR)}}\ . \tag{39}$$

This quantity is always less than unity, which reflects the fact that the QE of the free molecule is very high (nearly 1), and so the emission yield of the surface-adsorbed molecule can only be reduced by the additional nonradiative damping caused by the island. As expressed by Eq. (39), the electromagnetic resonance makes no contribution to the enhancement in the emission portion of the fluorescence from high QE molecules. Thus, attempts to use fluorescence as a probe of the spectral dependence of the emission portion of the electromagnetic resonance will be unsuccessful.[15,31] Furthermore, the only enhancement to the light scattering process will arise from the increased excitation rate, while the emission yield will, in fact, be decreased, resulting in an apparent additional damping. This accounts for the experimentally observed marked reduction in R_{F1} compared to both R_{RRS} and R_{RS}.

We can obtain an estimate for the effective quantum yield of the surface-adsorbed R6G molecules from this experiment. We restrict ourselves to those molecules adsorbed directly on the silver island, where the effects of the electromagnetic interaction are the strongest. For the fluorescence measurement with R6G, this is done by considering the value of R_{F1} measured on the island film on aluminum substrate $R_{F1}\sim 0.02$. We can then also use the measured value of R_{RS} to obtain an estimate for the average enhanced field intensity (~300) and the measured value of R_{RRS} to obtain an estimate of the average effects of the additional surface-induced damping on the excitation and transfer yield ($\sim 10^{-2}$). In so doing, we obtain an estimated fluorescence emission yield ratio of $\sim 10^{-2}$ for Eq. (39). These results suggest that $\Gamma_0^{(S,NR)}\approx 10^2\ \Gamma_0^{(S,R)}$. Since the dominant portion of the radiation that is emitted originates from the large induced dipole in the island, this result can also be viewed as an approximate measure of the radiative efficiency of a localized electronic plasma resonance, when excited by a molecular-emission dipole. A value of 10^{-2} for this efficiency is consistent with recent results obtained for excitation of a localized surface plasma resonance using a prism coupler.[32]

Finally, we consider BF, where the low QE means that $\Gamma_0^{(NR)}\approx 100\ \Gamma_0^{(R)}$. Since BF and R6G have similar $\Gamma_0^{(R)}$ (Ref. 25), BF can be expected to couple to the island plasma resonances to roughly the same extent as R6G. Thus, we expect the same effective yield for the surface-induced decay rate, which reflects the radiative

efficiency of the electronic plasma resonance. We can now express all the terms in the emission yield ratio in terms of $\Gamma_0^{(R)}$,

$$\frac{\Gamma_0}{\Gamma_0+\Gamma_0^{(s)}} \approx \frac{100\,\Gamma_0^{(R)}}{100\,\Gamma_0^{(R)}+|A(\omega')|^2\,\Gamma_0^{(R)}+100\,|A(\omega')|^2\,\Gamma_0^{(R)}} \cdot \approx 1 \tag{40}$$

Again we use our experimentally measured value for R_{RS} to obtain the average field intensity enhancement, and R_{RRS} to obtain the average effects of the surface-induced damping on the excitation rate and transfer yield. We obtain $R_{F1} \sim 3$ for BF, which is consistent with our measurements and correctly predicts the observed increase in the enhancement as the QE decreases. Despite the rapid decay of BF due to molecular nonradiative processes, the surface-induced decay plays a dominant role in the emission from BF on the island films, as is the case for R6G near the islands. Physically, the excitation is being coupled through the silver before it can nonradiatively decay within the molecule. The yield for the molecules on silver islands is then determined by the emission yield of the islands themselves, which is larger than the molecular yield for BF.

The qualitative agreement between our model and the data is very good, with the model correctly predicting the observed trends in the enhancement ratios of the various optical scattering processes. The model can now be applied to explain the results obtained in other environments. We note however, that a basic assumption made in all of our modeling is that the dominant mechanism involved in the enhancement process is electromagnetic in nature. There is considerable experimental evidence supporting this conclusion for evaporated rough silver surfaces, particularly those used under atmospheric conditions.[6,8,10] This evidence is based primarily on the spectral behavior of the excitation profiles and the long-range extent of the enhancement. However, there is a growing body of evidence that short range or "chemical" effects also contribute to the overall enhancement in SERS, particularly for surfaces electrochemically roughened[33] or prepared in high vacuum.[34] There is also some evidence that some form of chemical interaction between the adsorbate and the surface may be necessary in the case of island films.[35] While any possible additional mechanisms involved in the enhancement might change the detailed comparison of the theoretical expressions with our observations, the overall conclusions of the theory should not be affected. This is particularly true since we have introduced the surface-induced decay rates phenomenologically. It seems likely that any of the proposed chemical mechanisms will involve a strong interaction between the molecular energy levels and the surface, leading to substantial broadening of these levels.[36] Whenever the width of the molecular energy level plays a role in the damping of the optical scattering process, the relative enhancement of that process will be decreased, as shown by our theory. Thus, we believe that our interpretation, while based on the electromagnetic interactions, is in fact somewhat more general.

VI. CONCLUSIONS

In summary, we have presented measurements of the relative enhancement of a variety of optical scattering processes from molecules adsorbed on identical, well-characterized, silver-island films. We find a hierarchy of enhancements. Normal RS is enhanced by 10^5, RRS by 10^3, and fluorescence by ~ 10 for molecules with low QE and by $\lesssim 10^{-1}$ for molecules with high QE in their free state. These enhancement ratios were shown to have important spectroscopic implications. The relatively large increase in the RRS compared to fluorescence, particularly in the case of high QE fluorescence, can help eliminate fluorescence background problems for RRS spectroscopy. This feature has also been noted by other authors[37] and has already proved useful in work with biologically significant molecules adsorbed on metal colloids.[38] In addition, the increase in the enhancement of fluorescence with the decrease in the QE might have important consequences for fluorescence spectroscopy.

We have also presented a model that accounts for our experimental results by treating the optical scattering processes in a unified fashion, which includes the effects of the molecular resonance as well as that of the silver islands. This model correctly predicts the trends in the enhancement ratios that are observed, and also gives self-consistent agreement with the actual measured values.

We close by noting that the study of the wide variety of optical processes, all on optically identical surfaces, has allowed us to develop a detailed physical picture of the role of the electromagnetic interactions with the localized electronic plasma resonances in each portion of the optical scattering processes. The excitation of the plasma resonance by the incoming laser radiation results in an increase in the local field at the molecules, causing an increase in the excitation or absorption rate. Similarly, the response induced in the island by the emitting molecule results in a larger emission dipole, increasing the emission rate. However, both increased rates are offset by the additional damping caused by the absorptive portion of the response induced in the island by the molecules. Both this absorption and the island-induced increased emission dipole add an additional decay mechanism to the molecule which can compete with the other molecular decay channels. Thus, the increased absorption by the molecules is moderated due to the increased width of the absorbing state. Similarly, the emission yield can be decreased because of the competition with the absorption in the silver. Comparison of our model with our observations allows numerical estimates of each of these effects. The enhancement of normal RS suggests that the average excitation field intensity and the average emission dipole intensity are each increased by ~ 300. The enhancement of RRS suggests that when the molecule has a strong absorption that overlaps that of the metal plasma resonance, the excitation or absorption rate of the molecule is increased by ~ 30. The measured enhancement for fluorescence suggests that the increased damping of the silver further reduces the emission by adding an ad-

ditional decay channel during the thermalization process. Finally, comparison of dyes with high and low QE suggests that the increased plasma-resonance-induced emission rate dominates the molecular rates and has effective QE of $\sim 10^{-2}$. We note that this is a direct measurement of the effective QE of a localized plasma resonance, excited by a molecular emission dipole.

Finally, we emphasize that our goal in this paper was to investigate the enhancement of the optical scattering processes of molecules adsorbed on rough metal surfaces compared to the scattering of the same molecules in an inert environment. An alternate approach could have been to compare the scattering on rough and smooth metal surfaces. Indeed, there has been considerable effort in the study of the scattering from molecules near a smooth metal surface, particularly for fluorescence.[39] In this case, the details of the various mechanisms for energy transfer to the surface are rather well understood. While it is not our purpose in this paper to make the comparison between rough and smooth surfaces, we do point out one essential difference. In the case of a rough surface, the molecule can induce a macroscopic response in the rough metal, which, because of the localized nature of the roughness, can radiate. In contrast, because of the necessity of momentum conservation, any response induced in a smooth metal surface can not radiate. Thus, the effective QE of a molecule can be substantially increased on a rough surface as compared to a smooth metal surface.

ACKNOWLEDGMENTS

We thank T. J. Gramila, J. C. Chung, and M. S. Alvarez for their excellent technical assistance. Dr. H. Deckman obtained the electron micrographs of the films and Dr. R. Stephens performed the high sensitivity absorption measurements of the R6G coating. Two of us (JIG and AN) thank the U. S. –Israeli Binational Science Foundation for support.

[1]R. K. Chang and T. E. Furtak, *Surface-Enhanced Raman Scattering* (Plenum, New York, 1981).
[2]J. I. Gersten and A. Nitzan, J. Chem. Phys. 73, 3023 (1980).
[3]S. L. McCall, P. M. Platzman, and P. A. Wolff, Phys. Lett. A 77, 381 (1980).
[4]D. S. Wang, M. Kerker, and H. Chew, Appl. Opt. 19, 4159 (1980).
[5]C. Y. Chen and E. Burstein, Phys. Rev. Lett. 45, 1287 (1980).
[6]P. F. Liao, J. G. Bergman, D. S. Chemla, A. Wokaun, J. Mengailis, A. M. Hawrykuk, and N. P. Economu, Chem. Phys. Lett. 82, 355 (1981).
[7]J. E. Rowe, C. V. Shank, D. A. Zwemer, and C. A. Murray, Phys. Rev. Lett. 44, 1770 (1980).
[8]C. A. Murray, D. L. Allara, and M. Rhinewine, Phys. Rev. Lett. 46, 57 (1981).
[9]T. S. Yamaguchi, S. Yoshida, and H. Kimbara, Thin Solid Films 21, 173 (1974).
[10]D. A. Weitz, S. Garoff, and T. J. Gramila, Opt. Lett. 7, 168 (1982).
[11]J. G. Bergman, D. S. Chemla, P. F. Liao, A. M. Glass, A. Pinzuk, R. M. Hart, and D. H. Olson, Opt. Lett. 6, 33 (1981).
[12]J. I. Gersten and A. Nitzan, J. Chem. Phys. 75, 1139 (1981).
[13]D. S. Wang and M. Kerker, Phys. Rev. B 25, 2433 (1982).
[14]A. Nitzan and L. E. Brus, J. Chem. Phys. 75, 2205 (1981).
[15]A. M. Glass, P. F. Liao, J. G. Bergman, and D. H. Olson, Opt. Lett. 5, 368 (1980).
[16]G. Ritchie and E. Burstein, Phys. Rev. B 24, 4843 (1981).
[17]D. A. Weitz, S. Garoff, C. D. Hanson, T. J. Gramila, and J. I. Gersten, J. Lumin. 24/25, 83 (1981).
[18]D. A. Weitz, S. Garoff, C. D. Hanson, T. J. Gramila, and J. I. Gersten, Opt. Lett. 7, 89 (1981).
[19]S. Garoff, R. B. Stephens, C. D. Hanson, and G. K. Sorenson, Opt. Commun. 41, 257 (1982).
[20]J. T. Hall and P. K. Hansma, Surf. Sci. 71, 1 (1978).
[21]J. D. Langan and P. K. Hansma, Surf. Sci. 52, 211 (1975).
[22]S. Garoff, D. A. Weitz, T. J. Gramila, and C. D. Hanson, Opt. Lett. 6, 245 (1981).
[23]H. G. Craighead and A. M. Glass, Opt. Lett. 6, 248 (1981).
[24]C. F. Eagen, Appl. Opt. 20, 3035 (1981).
[25]J. M. Drake (private communication).
[26]D. L. Rousseau and P. F. Williams, J. Chem. Phys. 64, 3519 (1976).
[27]R. B. Stephens and G. K. Sorenson, Proc. Soc. Photo-Opt. Instrum. Eng. 276, 235 (1981).
[28]S. Mukamel and A. Nitzam, J. Chem. Phys. 66, 2462 (1977).
[29]C. K. Chen, A. R. B. DeCastro, and Y. R. Shen, Phys. Rev. Lett. 46, 145 (1981).
[30]Z. Kotler and A. Nitzan, J. Phys. Chem. 86, 2011 (1982).
[31]A. M. Glass, A. Wokaun, J. P. Heritage, J. G. Bergman, P. F. Liao, and D. H. Olson, Phys. Rev. B 24, 4906 (1981).
[32]J. Moreland, A. Adams, and P. K. Hamsma, Phys. Rev. B 25, 2297 (1982).
[33]A. Otto, J. Timper, J. Billman, and I. Pockrand, Phys. Rev. Lett. 45, 46 (1980).
[34]P. N. Sanda, J. M. Warlaumont, J. E. Demuth, J. C. Tsang, K. Christmann, and J. A. Bradley, Phys. Rev. Lett. 45, 1519 (1980).
[35]H. Seki, Solid State Commun. 42, 695 (1982).
[36]B. N. J. Persson, Chem. Phys. Lett. 82, 561 (1981).
[37]C. Y. Chen, I. Davoli, G. Ritchie, and E. Burstein, Surf. Sci. 101, 363 (1980); K. Caron, J. Haushalter, N. Levinger, T. Cotton, and R. P. Van Duyne (private communication to A.N.).
[38]M. E. Lippitsch, Chem. Phys. Lett. 79, 224 (1981).
[39]See, for example, R. R. Chance, A. Prock, and R. Silbey, in *Advances in Chemical Physics*, edited by I. Prigogine and S. A. Rice (Wiley, New York, 1978), Vol. 37, p. 1, and references therein.